NUREG/CR-4240 Vol. I
ANL-85-23 Vol. I

NUREG/CR-4240 Vol. I
ANL-85-23 Vol. I

PHYSICS OF REACTOR SAFETY

Quarterly Report
January – March 1985

ARGONNE NATIONAL LABORATORY, ARGONNE, ILLINOIS
Operated by THE UNIVERSITY OF CHICAGO

Prepared for the Office of Nuclear Regulatory Research
U. S. NUCLEAR REGULATORY COMMISSION
under Interagency Agreement DOE 40-550-75

Available from

Superintendent of Documents
U. S. Government Printing Office
Post Office Box 37082
Washington, D.C. 20013-7982

and

National Technical Information Service
Springfield, VA 22161

NUREG/CR-4240 Vol. I
ANL-85-23 Vol. I

(Distribution
Code: R7)

ARGONNE NATIONAL LABORATORY
9700 South Cass Avenue
Argonne, Illinois 60439

PHYSICS OF REACTOR SAFETY

Quarterly Report
January-March 1985

Applied Physics Division
Components Technology Division

May 1985

Previous reports in this series

ANL-84-35 (I)	January-March 1984
ANL-84-35 (II)	April-June 1984
ANL-84-35 (III)	July-September 1984
ANL-84-35 (IV)	October-December 1984

Prepared for the Division of Accident Evaluation
Office of Nuclear Regulatory Research
U.S. Nuclear Regulatory Commission
Under Interagency Agreement DOE 40-550-75

NRC FIN Nos. A2015 and A2045

PHYSICS OF REACTOR SAFETY

Quarterly Report
January-March 1985

ABSTRACT

This Quarterly progress report summarizes work done during the months of January-march 1985 in Argonne National Laboratory's Applied Physics and Components Technology Divisions for the Division of Reactor Safety Research of the U.S. Nuclear Regulatory Commission. The work in the Applied Physics Division includes reports on reactor safety modeling and assessment by members of the Reactor Safety Appraisals Section. This will be the final Quarterly Report on this activity as funding for it has now been exhausted. Work on reactor core thermal-hydraulics is performed in ANL's Components Technology Division, emphasizing 3-dimensional code development for LMFBR accidents under natural convection conditions. An executive summary is provided including a statement of the findings and recommendations of the report.

FIN No.	Title
A2015	Reactor Safety Modeling and Assessment
A2045	3-D Time-Dependent Code Development

TABLE OF CONTENTS

LIST OF FIGURES

LIST OF TABLES

Executive Summary

A parametric study of reactivity feedback from irradiated pin failure in unprotected slow TOP accidents in oxide-fueled LMFBR's has been completed. Results have been incorporated in a paper to be presented at the Knoxville Fast Reactor Safety Meeting. This study represents a further development of work originally undertaken in connection with CRBR licensing. A mid-plane failure location was assumed in order that the maximum potential for an autocatalytic power rise in the reactor could be assessed. The PLUTO2 module of the SAS4A fast reactor accident analysis code was used. The most important parameters varied were those concerned with fuel-to-coolant and coolant-to-clad heat transfer. Varying the fuel-to-coolant heat transfer parameters strongly affects determination of fuel flow regime. Increasing such heat transfer tends to produce an earlier transition from particulate to annular fuel flow, which reduces fuel sweepout. Increased coolant to clad heat transfer retards this transition, increasing sweepout. Sodium vapor production from lower slug reentry was found to have an important effect in increasing sweepout in most cases.

Khalil and Yarlagadda in 1984 published comparative LOF HCDA studies using the SAS4A code for several 1000 MWe oxide-fueled LMFBR concepts including conventional homogeneous and heterogeneous designs, and a "quasi-homogeneous" design in which incoherence in sodium boiling and fuel pin failure was achieved by using driver pins of two different diameters, arranged in alternating annuli. It was found in their study that peak net reactivity and power and total energy release were less with the new design than with either of the other two, and that the advantage of the heterogeneous design over the homogeneous was less than would be expected from previous studies. It was determined by analysis of their results that the advantage in going to a heterogeneous design is much less with SAS4A because of the positive inpin fuel motion calculated by the LEVITATE module for higher power channels. This greatly reduces the advantage of eliminating LOF-TOP effects in the lower power channels. For the quasi-homogeneous design, LOF-TOP effects in the lower power (large pin) assemblies are not completely eliminated, but are delayed to the point that they can be effectively offset by negative Doppler and axial expansion effects. The total positive ramp rate from fuel motion, sodium voiding, and clad motion is not much different up to the time of attainment of peak net reactivity for the quasi-homogeneous and heterogeneous cases, but the total negative ramp rate from the Doppler effect and axial fuel expansion is less for the heterogeneous case mainly because of the positive effect from expansion of the inner blanket fuel, which has a negative worth. In evaluating these results, it should be kept in mind that some of the advanced modeling features in SAS4A are still in an early stage of validation.

In the single-phase COMMIX development, the efforts were continued toward cleaning and documentation of the COMMIX-1B code. In the area of two-phase COMMIX development, several boundary condition options have been added and a simulation was performed to validate the slip model.

I. REACTOR SAFETY MODELING AND ASSESSMENT

(A2015)

A. TOP Studies with SAS4A/PLUTO2 (H. H. Hummel and P. A. Pizzica)

We have now completed work on a paper to be presented at the Knoxville Fast Reactor Safety Meeting in April 1985 by H. H. Hummel and P. A. Pizzica entitled "Reactivity Feedback from Irradiated Pin Failure in Unprotected Slow TOP Accidents in LMFBR's". Here we briefly describe the most important results of this paper and also discuss some aspects of this work not really covered in the paper.

The example chosen is a 10 ¢/s TOP accident in the CRBR EOC-3 core, using the PLUTO2 module in the SAS4A code system. Parameters varied in the present study included Cho-Wright FCI parameters, CIVOID (a PLUTO2 input variable defining the sodium void fraction at which a transition is made from single-phase to two-phase correlations for sodium/clad heat transfer and friction), fuel/sodium heat transfer in the annular flow regime, and pin failure pressure.

The Cho-Wright formula for the particulate flow fuel/coolant heat transfer coefficient h per unit area of fuel is

$$h = C \frac{k_{fu}}{R_p} (NaVF)^X$$

where

C is a constant set at 1.0 in the present work,

k_{fu} is fuel thermal conductivity

R_p is fuel particle radius

NaVF is the sodium liquid volume fraction in the coolant channel, and

X is assigned a value of 1 or 2.

About two years ago we carried out a similar but less comprehensive study in support of CRBR licensing activities[1]. At that time reference or base case parameters chosen were X = 2, failure pressure 20.0 MPa, CIVOID = 0.5, particle radius R_p = 170 μm, and fuel thermal conductivity k_{fu} = 3.6 watts/m-K. Also the maximum heat transfer coefficient between fuel and liquid sodium droplets in the annular fuel flow regime was set at 10^5 watts/m^2-K.

When undertaking the present studies we made several changes in reference assumptions, which had the effect of drastically reducing fuel sweepout in the early part of the transient, up to about 50 ms, as discussed in the paper. One such change was to raise k_{fu} from 3.6 to 5.6 watts/m^2/K, which seemed to be more consistent with recent experimental results for molten fuel[2]. The resultant increase in FCI heat transfer had the effect of hastening the transition from particulate to annular flow, reducing fuel sweepout.

Another change in reference assumptions was to set CIVOID = 0 instead of 0.5, as we felt uncertain about the validity of using single-phase correlations for heat transfer and friction over such a wide range of sodium void fractions. This was found to cause a considerable reduction in early sweepout, apparently for the same reason that an increase in FCI strength did: the resultant decrease in sodium cooling early in the transient hastens the transition from particulate to annular fuel flow. This seemed to be inconsistent with our earlier results[1], in which less sweepout was obtained when CIVOID was set high enough that the transition from single-phase to two-phase correlations should never have occurred. An explanation for this apparent discrepancy was provided by the discovery that due to a bug in the earlier version of the code, CIVOID rather than 1-CIVOID was being compared to the sodium void fraction to determine when the transition should occur. This would not affect the transition if CIVOID was set at 0.5, but inputting a high value of CIVOID was actually resulting in CIVOID = 0 being used in the code.

The value of CIVOID was set at 0.5 as a result of the analysis of the L8 experiment by Bowers et al[3]. In order to see how well this parameter is determined by this experimental comparison, we have used the same standalone version of PLUTO2 used in the original work to carry out additional parameter studies, with results given in Table I. In this table, calculated and experimental fuel worth as a function of time are given normalized to an initial value of unity. The decrease in fractional worth shows the effect of fuel sweepout. The positive reactivity effect from inpin motion to the assumed midplane failure point is calculated to be small for L8. The fractional fuel worth is presented as a function of three parameters: k_{fu}, CIVOID, and maximum annular flow fuel/coolant heat transfer. The higher value for this last parameter was used by Bowers et al. The lower value, essentially zero, was selected as the reference value in the Knoxville paper. The value of 2.4 watts/m-K for k_{fu} was used by Bowers et al. We used 3.57 in our previous work, while 5.6 was adapted as the reference value in the Knoxville paper.

The results in Table I do not indicate a great sensitivity of calculated fuel sweepout to CIVOID for the L8 experiment, particularly for the choices of k_{fu} and annular flow fuel/sodium heat transfer made by Bowers et al. A slightly better agreement with experiment is obtained with the higher value of CIVOID, but this does not appear to provide a very firm basis for selecting this parameter. We found a greater sensitivity of sweepout to CIVOID for the prototypical TOP case, apparently because the clad is colder earlier in the transient than it was in L8, a LOF-TOP simulation, so that the cooling effect of sodium/clad heat transfer on the sodium is consequently greater.

In the Knoxville paper we found that for the base case, sufficient fuel sweepout to produce a total negative feedback effect was not obtained until reentry of the lower sodium slug occurred 55 ms after pin failure, resulting in increased sodium vapor production. Such reentry was found to be essential in producing sweepout in a number of the cases with low initial sweepout, with the resultant "spike" in sodium vapor pressure appearing 50 to 80 ms after pin failure. Factors affecting this reentry and the way it acts to increase fuel sweepout are discussed in the following.

When the pin fails, the contribution to the coolant channel pressure from fission gas is high enough to rapidly reverse the coolant flow below the

failure site. After about 5-10 ms, substantial amounts of sodium vapor pressure are produced in the coolant channel as well and this persists as the fission gas pressure declines so that the lower slug velocity remains negative for 30-50 ms after failure, depending on the case parameters. Eventually the voided interaction zone in the coolant channel has expanded so much that fission gas pressure is reduced to a maximum of a few atmospheres even where it has accumulated near the lower slug and in many places in the interaction zone it is negligible. Sodium vapor pressure is reduced eventually as well because of the expansion of the interaction zone and the cooling of the fuel, and because much of the fuel is in an annular flow regime instead of particulate flow and as a result the heat transfer from fuel to sodium is greatly reduced. There is also condensation on cold cladding as the slug proceeds downwards.

When the lower sodium slug begins to move upward several phenomena tend to enhance fuel sweepout. The lower sodium slug starts to move upward when the fuel near the interface is still moving downward and even later, when the fuel has reversed direction, the sodium often moves upward more rapidly than the fuel. The result of this is that, since the interaction zone is defined by the limits of the fuel, some liquid sodium from the end of the lower slug becomes mixed into the interaction zone. As the slug moves upward, the newly added sodium from the slug, the liquid sodium which was already at the lower end of the interaction zone, and the fission gas which had accumulated at the lower slug interface during the downward motion of the slug are all pushed ahead of the slug interface. This compresses the fission gas since the void fraction in the several nodes above the interface decreases, thus increasing the contribution of fission gas to the total pressure. Since the lowest nodes in the interaction zone are almost always in the particulate fuel flow regime, this fuel can more readily heat the sodium than can fuel in the annular flow regime. Frequently a node towards the lower interface changes from annular to particulate flow as the sodium volume fraction increases and this enhances the heat transfer from fuel to sodium. Also the fuel to sodium heat transfer increases simply by virtue of the fact that the sodium volume fraction increases ahead of the interface.

The result of this process is a significant increase in pressure in the coolant channel above the lower slug interface and in the vicinity of the failure. Fission gas can make a substantial contribution to this increase in pressure although the more significant contribution is from sodium vapor. The fission gas pressure at the interface often plays a role in moving sodium up into hotter nodes above by creating a larger pressure gradient immediately above the interface than sodium vapor would alone. This pressure increase is sustained over tens of milliseconds and produces a pressure gradient upward in the coolant channel of at least several atmospheres at the time when the pin pressure is spent and can contribute no longer to channel hydrodynamics. This produces a significant redistribution of channel fuel upward and a substantial increase in sweepout. Our studies showed that without this reentry induced increase in sweepout in many cases the attainment of a negative net reactivity would take substantially longer and may very well be unlikely in less than 100 ms after failure.

The existence of this lower slug reentry phenomenon has not been confirmed experimentally, possibly because of the limitations of TREAT accident simulation. Even if such a delayed increase in fuel sweepout was

observed in an experiment, it would not be easy to assign a cause to it and to correlate precisely the increased sweepout with the upward motion of the lower sodium slug. However, the phenomenon does seem plausible for the following reasons. Eventually the pressure inside the fuel pin must be spent without further fuel melting into the cavity with the relatively low power conditions of a 10 ¢/s ramp. Cavity pressures in these circumstances are usually below 0.5 MPa. Further channel pressure contributions from this source are not possible. Sodium vapor pressure in the coolant channel must eventually drop to low values because of the expansion of the interaction zone, the prevalence of annular fuel, the cooling of the fuel and the reduction of heat transfer due to a lower sodium volume fraction. Even if these mechanisms are not sufficient to lower the sodium vapor pressure, the cold cladding revealed as the slug moves downward provides an ample heat sink for condensation. Therefore, with the full pump head of TOP conditions, eventually the lower slug will reverse direction. It seems reasonable that there would be some accumulation of fission gas and liquid sodium in advance of the slug as it moves upwards since the pressure gradient is downward in the interaction zone toward the lower slug interface as it is expelled. Also, there is a source of liquid sodium from the leading edge of the slug as it reenters and mixes with fuel it overtakes. These considerations seem to indicate that a reentry-induced increase in fuel sweepout is very likely unless channel pressure remains high, in which case adequate sweepout should occur even in the absence of lower slug reentry.

B. Analysis of Oxide-Fueled LMFBR LOF Calculations Performed by Khalil and Yarlagadda (H. H. Hummel)

Last year Khalil and Yarlagadda[4] published comparative results of LOF HCDA calculations, performed using the SAS4A code[5], for several 1000 MWe oxide-fueled reactor concepts. These included conventional homogeneous and radially heterogeneous design, and also a new "quasi-homogeneous" concept in which sodium boiling and fuel failure incoherence is achieved by using two types of driver assemblies, differing in pin diameter and number of pins. Satisfactory results were achieved with the "R6A" design, in which the ratio of large to small pin diameter is 1.284. There are six core regions containing alternately large (LPA) and small (SPA) pin assemblies, with the core layout resembling a conventional heterogeneous design. The incoherence in sodium boiling and in fuel failure in the R6A design was found to be quite effective in reducing energy release in an unprotected LOF accident compared to that in the homogeneous design. A further interesting result was that energy release was also less than that in the heterogeneous design, which was not as much less than that of the homogeneous design as might have been expected from previous analyses with the SAS3D code. The present work, one purpose of which is to explore the reasons for this result, is based on a study of the SAS4A output results for these cases, made available by courtesy of the authors.

In the SAS3D code, pin failure in higher power channels, in which extensive sodium voiding is expected to occur, is treated by the SLUMPY module. In this model, for axial pin nodes in which radial sodium voiding and clad melting have occurred, pin failure triggered by a criterion such as attainment of 0.50 fuel melt fraction leads to formation of a totally disrupted region in which fuel motion is treated by one-dimensional compressible hydrodynamics. Fuel below the disrupted region remains

stationary, while fuel above can fall by gravity into the disrupted region. The disrupted region fuel can move into the coolant channels of the fuel above and below. There is no provision for treatment of fuel motion within the intact parts of these pins. Fuel motion reactivity effects in SLUMPY are produced by motion of the disrupted region fuel and of the upper intact fuel. Considerable positive ramp rates can be attained in SLUMPY from gravity slumping of fuel under certain circumstances. There is evidence, however, that this is unrealistic for irradiated fuel, as only a small amount of trapped fission gas seems to be sufficient to prevent much slumping from occurring. Fuel dispersal leading to accident termination is produced in the last resort by fuel vapor pressure. It is also possible to calculate earlier fuel dispersal by steel vapor pressure, fission gas, and sodium vapor sweepout. However, we feel that the modeling of these effects in SAS3D is for the most part too crude to take them to account, and in work for the NRC usually assumed dispersal by fuel vapor pressure for conservatism. For slower transients in which several seconds elapse between boiling initiation and fuel disruption, motion of molten clad can occur, causing a significant reactivity effect.

Pin failure in lower power channels, in which sodium voiding is less extensive, is treated in SAS3D by the SAS/FCI module (replaced by EPIC in SAS3D/EPIC). In this case, the clad is assumed to remain intact except for local failures that permit ejection of a mixture of fuel and fission gas. A high sodium voiding ramp rate, much higher than results from boiling, can occur as a result of molten fuel coolant interaction (FCI). A large positive fuel motion ramp rate can occur from molten fuel motion inside the pin to a core midplane failure point under fission gas pressure. If the failure point is at about 0.7 of the core height or higher, this effect becomes negative.

These high ramp rates correspond to the original LOF-TOP situation. According to the original scenario, development of LOF-TOP conditions, and of consequent large energy release, is prevented in a heterogeneous design by lowering the core sodium void worth to the point that extensive sodium voiding is necessary for an approach to prompt critical and a substantial power rise. As a result, there would not be a significant fraction of the core in which development of LOF-TOP conditions was possible.

In SAS4A, higher power channels in a LOF accident are treated by the LEVITATE module. This also provides for total pin disruption, as in SLUMPY, but in axial nodes in which significant fuel melting has occurred but clad melting is not complete, motion of fuel and fission gas within the pin and of fuel, fission gas, and sodium vapor, (or vapor/liquid mixture) in the coolant channel is provided for. This inpin fuel motion in the upper and lower intact pin regions will, in general, be toward the axial midplane, producing a positive reactivity effect. Lower power channels are treated with PLUTO2, which assumes intact clad except for local failures, as in SAS/FCI. A transition from PLUTO2 to LEVITATE occurs in a channel if sufficient clad melting occurs as specified by an input parameter.

To aid in the analysis of the Khalil-Yarlagadda results, ramp rates for various reactivity components as a function of time have been listed in Tables II, III, and IV for homogeneous, quasi-homogeneous, and heterogeneous cases, respectively. In Table V, values of various reactivity components at peak net reactivity have been given.

The results in Table II show that attainment of prompt critical conditions in the homogeneous case is caused by boiling voiding, consistent with the total core void worth. Comparison of the void reactivity of the lower power channels at peak net reactivity compared to the total core void worth for these channels shows that they are not extensively voided at this time, so that there is a considerable potential for LOF-TOP development. This in fact occurs, as shown by the large ramp rates for sodium voiding and fuel motion which develop in the lower power channels. LOF-TOP development is exacerbated by the fuel motion calculated in LEVITATE. The transient is turned around primarily by the Doppler effect, but not without development of net reactivity far above prompt critical and a consequent large energy release. Shutdown from fuel dispersal occurs too late to prevent this because of the high rate of reactivity insertion. Because of the rapid power rise in this case, clad motion is not a relevant factor. The large clad motion indicated at the end of the transient corresponds to steel motion calculated in LEVITATE.

The feedback history for the quasi-homogeneous case shows the beneficial effect of increased incoherence in boiling and fuel failure introduced by the use of the two pin sizes. LOF-TOP effects still develop in the LPA channels but so late in the transient that negative fuel motion effects are starting to come in, and net reactivity does not rise as much above prompt critical as for the homogeneous case. The inpin fuel motion in the LEVITATE (SPA) channels in the earlier part of the transient is not too much different in the two cases, but the delay in introduction of LOF-TOP effects in the quasi-homogeneous case makes it possible for Doppler and axial expansion feedback to counteract this positive reactivity input more effectively. Clad motion is more evident in this case because of the slower power rise but is still not a significant factor.

For the heterogeneous case, it is evident from the results in Table IV that success has been achieved in reducing the positive sodium voiding ramp because of the reduced sodium void worth. Also, the possibility of LOF-TOP development is eliminated, as core voiding is substantially complete at maximum net reactivity. A positive inpin fuel reactivity in the LEVITATE channels comparable to that in the other two cases is calculated. The fuel motion reactivity given in Table IV is substantially all from this source. In Table V, for the heterogeneous case, "higher" and "lower" power channels refer to driver channels only. Values are not given for the inner blanket channels except that their worth is included in the totals and also a value is given for the inner blanket contribution to axial fuel expansions. It is seen from Tables III and IV that the total positive reactivity ramp rate from sodium voiding plus fuel and clad motion tends to be less in the heterogeneous case than in the quasi-homogeneous case until fairly late in the transient. The peak net reactivity and power become greater in this case because of a reduction in the negative feedback from axial fuel expansion and the Doppler effect. In the former case, it is clear that this results from a positive ramp rate from expansion of the inner blanket channels, which have a negative fuel worth. This effect would not be too important in the absence of the inpin fuel reactivity effect but becomes significant in the present case. The increased Doppler ramp rate for the quasi-homogeneous LPA in the early part of the transient over that for the heterogeneous inner blanket assemblies, which have about the same Doppler coefficient, is apparently due to the greater heating of the LPA.

Some points about SAS4A modeling should be kept in mind in considering the Khalil-Yarlagadda results, as follows:

1. Although the modeling of inpin reactivity in LEVITATE seems reasonable, it is not yet really supported by anything much in the way of experimental evidence. There might be a question as to whether this type of fuel motion inside the pin clad would actually occur in a few milliseconds, and whether the clad would be sufficiently intact to channel fuel toward the center of the core. Fission gas pressure might not be generated as rapidly as required to produce the calculated motion. It is not too clear how this phenomenon would be investigated experimentally. Transients this rapid are not possible with TREAT, so that some other facility would be required.

2. Clad motion makes an important contribution to attainment of prompt criticality in the heterogeneous case, although the rate of addition is fairly slow. There is still considerable uncertainty in the modeling of this effect, although high ramp rates from it seems unlikely. A reduction in the clad motion reactivity contribution would make the heterogeneous case look considerably better.

3. The LOF-TOP reactivity contribution in the homogeneous case may be somewhat exaggerated by use of a melt fraction pin failure criterion. Use of a burst pressure criterion may reduce the positive fuel motion contribution from this source by raising the failure point to above the core midplane.

4. Final shutdown from fuel dispersal is achieved in these calculations by generation of steel vapor pressure in regions of total pin disruption, in which fuel and steel are homogenized. Although this seems reasonable, it is not really supported as yet by any experimental evidence that substantial steel vaporization would occur under these circumstances in a few milliseconds. For this reason, this assumption seems somewhat speculative and a reliance instead on fuel vapor pressure would be easier to defend. The effect of the resulting delay might not be very important for total energy release in this present case.

II. THREE-DIMENSIONAL CODE DEVELOPMENT FOR CORE THERMAL-HYDRAULIC ANALYSIS OF LMFBR ACCIDENTS UNDER NATURAL CONVECTION CONDITIONS

A2045

A. INTRODUCTION

The objective of this program is to develop computer programs (COMMIX and BODYFIT) which can be used for either single-phase or two-phase thermal-hydraulic analysis of reactor components under normal and off-normal operating conditions, especially under natural circulation. The governing equations of conservation of mass, momentum, and energy are solved as a boundary value problem in space and as an initial value problem in time.

COMMIX is a three-dimensional, transient, compressible flow computer code for reactor thermal-hydraulic analysis. It is a component code and uses a porous medium formulation to permit analysis of a reactor component/multicomponent system, such as fuel assembly/assemblies, plenum, piping system, etc., or any combination of these components. The concept of volume porosity, surface permeability, and distributed resistance and heat source (or sink) is employed in the COMMIX code for quasicontinuum thermal-hydraulic analysis. It provides a much greater range of applicability and an improved accuracy than subchannel analysis. By setting volume porosity and surface permeability equal to unity, and resistance equal to zero, the COMMIX code can equally handle continuum problems (reactor inlet or outlet plenum, etc.).

B. COMMIX-1A, COMMIX-1B, SINGLE-PHASE CODE DEVELOPMENT (F. F. Chen, H. N. Chi, H. M. Domanus, R. C. Schmitt, V. L. Shah)

In this quarter, the following efforts were continued in the process of documentation and release of COMMIX-1B:

i. cleaning of the code,

ii. preparation of input and user instructions, and

iii. rerunning the several sample problems to ensure no errors have been introduced.

During the cleaning of the code, several inconsistencies and bugs were detected. One inconsistency was in the calculation of the heat transfer coefficient using the wall function of the 2-equation turbulence model for fluids having a Prandtl number of the order of unity. All of the inconsistencies and bugs detected during cleaning have been corrected. A section of the skew-upwind differencing model has been rewritten for better organization and increased efficiency of the calculations.

Efforts will be continued to clean and test the code to eliminate as many bugs as possible.

C. DEVELOPMENT OF COMMIX-2 (T. H. Chien and W. T. Sha)

C.1 Boundary Condition Options

During this quarter, the two-phase boundary conditions have been implemented in the COMMIX-2 SPM (Separated Phase Model) to account for the boundary conditions for each phase when the two-phase region spreads up to the boundary surfaces.

Similar to the COMMIX-2 HEM (Homogeneous Equilibrium Model), six types of temperature boundary condition options,

- constant temperature,
- transient temperature,
- constant heat flux,
- transient heat flux,
- adiabatic surface, and
- duct wall,

and two types of pressure boundary conditions options

- constant pressure, and
- transient pressure

are available in COMMIX-2 SPM. However, for the velocity boundary conditions, only the option of the continuative mass flow is considered when the two-phase region spreads up to the boundary surfaces.

The continuative mass flow at the boundary surfaces is derived from the mass conservation equations of the liquid and vapor phase at the boundary adjacent fluid cells, that is

Liquid phase

$$\frac{\partial \rho_\ell'}{\partial t} + \nabla \cdot \left(\rho_\ell' \vec{u}_\ell\right) = - \dot{M}''' \tag{1}$$

Vapor Phase

$$\frac{\partial \rho_g'}{\partial t} + \nabla \cdot \left(\rho_g' \vec{u}_g\right) = \dot{M}''' \tag{2}$$

where

ρ_ℓ' is the macroscopic density of the liquid phase,

ρ_g' is the macroscopic density of the vapor phase,

$\vec{u}_\ell$ is the velocity vector of the liquid phase,

$\vec{u}_g$ is the velocity vector of the vapor phase, and

$\dot{M}'''$ is the vapor mass generation rate per unit volume.

Similar to the HEM version, only the one-dimensional case of Eqs. 1 and 2 is assumed at the boundary surfaces.

In programming, for consistency and simplicity, we add the suffixes "L" and "G" to the boundary variables that we used in the COMMIX-2 HEM to represent the boundary variables of the liquid and vapor phases respectively. The new variables used in COMMIX-2 HEM are summarized as

VELBNL = Velocity of liquid phase at boundary

VELBNG = Velocity of vapor phase at boundary

RLBL = Macroscopic density of liquid phase at boundary

RLBG = Macroscopic density of vapor phase at boundary

TLBL = Temperature of liquid phase at boundary

TLBG = Temperature of vapor phase at boundary

HLBL = Enthalpy of the liquid at boundary

HLBG = Enthalpy of the vapor phase at boundary, and

XQBN = Thermodynamic quality of the vapor phase at the boundary.

Implementation of the two-phase boundary conditions has been completed. The code has been used to test a sample problem with the two-phase conditions at the outlet surface and the solution converges.

C.2 Debugging and Testing

After completion of implementation of the two-phase boundary condition in the Separated Phase Model, our efforts were continued toward debugging and testing the interfacial drag force model.

To test the two-phase boundary condition when the two-phase flow spreads to the boundaries, we also simulated the steady-state steam-water void fraction experiment by Thom et al., as described in the previous section, with the Separated Phase Model. During the calculation, the interfacial drag force function between the vapor phase and the liquid phase was taken to be constant. Pressure at both the inlet boundary and the outlet boundary were specified according to the values obtained in the Slip Model. We obtained a converged solution where the void fraction ranged from $\alpha = 0.12$ at $z = 0.9$ m to $\alpha = 0.61$ at $z = 1.5$ m. These values are much lower than the corresponding experimental values as shown in Fig. 1.

The results may be improved once the interfacial drag force model is completely debugged.

C.3 Verification of Slip Model

As part of an investigation of subcooled boiling, Thom et al.[6] measured the void fraction in a steam-water mixture flowing in an electrically heated tube. Single phase water was introduced at the inlet of the test section, and bulk or saturated boiling was present near the test section outlet.

The test section tube had a heated length of 1.524 m (5 ft) with an inside diameter of 9.754 mm (0.384 in). Density measurements were made with a Thulium-170 gamma source, and these measurements were used to compute local void fractions. Density measurements were made every 4.45 cm (1.75 in) between 0.273 m (10.75 in) from the inlet and 0.139 m (5.5 in) from the outlet.

The experimental data reported by Thom et al. included the void fraction profile, the inlet water temperature, the mass flux, the heat flux, and pressure. The location of the reported pressure was not given, so it was assumed that this was the outlet pressure. Any error resulting from this assumption is assumed to be small because the pressure drop across the test section is less than 3.445×10^4 Pa (5 psi).

One experiment (Test No. 12) was simulated with the COMMIX-2 code. The pressure for this run was 5.2724×10^6 Pa (764.7 Psia). The uniform heat flux was 9.053×10^5 W/m^2 (2.87×10^5 Btu/ft^2-hr), the mass flux was 9.53×10^2 kg/(m^{2}s) (7.03×10^5 lb/ft^2-hr) and the inlet temperature was 225.56°C (438°F). This inlet temperature corresponds to an inlet subcooling of 41.7°C (75°F).

The 1.524 m (5 ft) heated test section was modeled in one dimension using 12 equally sized 0.127 m nodes. The analysis of this problem was performed with the steady-state option in COMMIX-2. A very large time step was used, typically $\Delta t = 100$ s which is about 10^3 larger than the transport time through a computational mesh. The water properties package is based on Agee's functional fits for density enthalpy and temperature.[7]

Initially the tube was assumed to be filled with subcooled stagnant water at a uniform pressure of 5.27×10^6 Pa and 255.56°C. The boundary conditions at the inlet maintained the liquid phase velocity at 1.14 m/s (3.74 ft/s) and the liquid phase temperature at 225.56°C (438°F) which corresponds to a liquid phase enthalpy of 9.7×10^5 J/kg (417 Btu/lb). The outlet pressure was maintained at 5.27×10^6 Pa (764.7 psia). The wall heat flux was converted to a volumetric heat source.

Several runs were performed to assess the slip model and the two-phase flow friction multiplier which uses the Lockhart-Martinelli correlation.[8] This approach has been found suitable for not only water, but also sodium two-phase pressure drop.[9] The experimental void fraction data and the void fraction computed by the COMMIX-2 code are shown in Fig. 1 for two slip ratios, $H_z = 1$ and $H_z = 2$. Clearly, the case of $H_z = 1$ agrees better with the data. The effect of the slip ratio is quite pronounced causing the void fraction to be lowered as the slip ratio is increased. A more mechanistic slip ratio model may yield better results. Both cases begin boiling later than the data (about 0.4 m vs. about 0.2 m) because thermodynamic equilibrium between the phases is assumed. Therefore, subcooled boiling is not predicted. Clearly, the data show the subcooling persists only for a short distance (about 0.2 m) and then saturated boiling begins.

REFERENCES

1. Physics of Reactor Safety Quarterly Report for January-March 1983, NUREG/CR-3359 Vol I, ANL 83-11 Vol I.

2. J. K. Fink and L. Liebowitz, private communication.

3. C. H. Bowers, et al., "Analysis of TREAT Tests L7 and L8 with SAS3D, LEVITATE and PLUTO2," Proceedings of Specialists' Workshop on Predictive Analysis of Material Dynamics in LMFBR Safety Experiments, Los Alamos Scientific Laboratory, Los Alamos, NM, March 13-15, 1979, p. 153.

4. H. Khalil and B. S. Yarlagadda, "An Evaluation of the Core Physics and Safety Characteristics of a Quasi-Homogeneous LMFBR Concept," Topical Meeting on Reactor Physics and Shielding, Chicago, IL, 1984.

5. H. U. Wider, et al., "Status and Validation of the SAS4A Accident Analysis Code System," Proceedings of the LMFBR Safety Topical Meeting, July 19-23, 1982, Lyon, France, p. II-13.

6. J. R. Thom, W. M. Walker, T. A. Fallon, G. F. S. Reising, "Boiling in Sub-Cooled Water During Flow Up Heated Tubes or Annuli," Proc. Instn. Mech. Engrs., 180 Pt 1 2C, pp. 226-246 (1965-1966).

7. L. J. Agee, "An Analytical Method of Integrating the Thermo-Hydraulic Conservation Equations," Nuclear Eng. and Design, 42, pp. 195-208 (1977).

8. R. W. Lockhart and R. C. Martinelli, "Proposed Correlation of Data for Isothermal Two-Phase Two-Component Flow in Pipes," Chemical Eng. Progress, 45 (1949).

9. C. Savatteri and H. M. Kottowski, "Two-Phase Flow Metal Boiling Characteristic," Heat Transfer in Nuclear Reactor Safety (S. G. Bankoff and N. H. Afgan, Eds.,), pp. 259-286, Hemisphere Publ. Corp., Washington (1982).

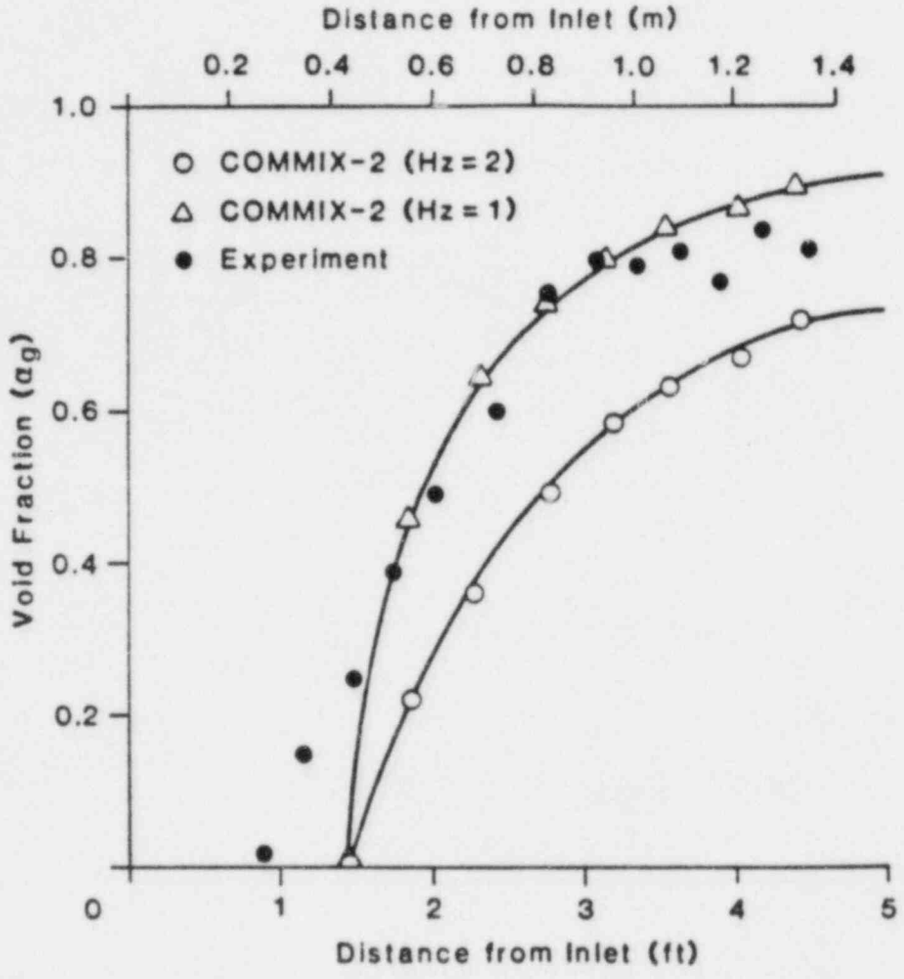

Fig. 1 Comparison of Experimental and Computed Steady-State Void Fraction for Test No. 12, Thom et al.

TABLE I. Fuel Worth in L8 Experiment as Fraction of Original Value Calculated with Standalone PLUTO2 Code for Varying k_{fu} and CIVOID. Fuel Particle radius 170 μm, X = 2.

Time, ms.	CIVOID=0 k_{fu}, watts/m-K			CIVOID=05 k_{fu}, watts/m-K			Exp
	2.4	3.57	5.6	2.4	3.57	5.6	
	Annular Flow Na/Fuel Heat Transfer 500 watts/m-K						
10	0.985	0.985	0.986	0.984	0.983	0.983	1.01
20	0.966	0.972	0.974	0.961	0.963	0.964	0.99
30	0.960	0.969	0.971	0.952	0.954	0.955	0.96
40	0.957	0.969	0.971	0.951	0.951	0.950	0.93
50	0.950	0.968	0.960	0.947	0.944	0.945	0.90
60	0.933	0.957	0.944	0.933	0.928	0.936	0.88
70	0 908	0.940	0.923	0.913	0.908	0.919	0.88
80	0.890	0.927	0.908	0.897	0.893	0.904	0.88
	Annular Flow Na/Fuel Heat Transfer 10^5 watts/m-K						
10	0.985	0.985	0.986	0.984	0.983	0.983	1.01
20	0.966	0.973	0.973	0.961	0.963	0.964	0.99
30	0.956	0.967	0.970	0.951	0.954	0.955	0.96
40	0.955	0.963	0.968	0.952	0.952	0.951	0.93
50	0.951	0.945	0.959	0.948	0.946	0.943	0.90
60	0.938	0.941	0.946	0.922	0.932	0.930	0.88
70	0.921	0.926	0.931	0.916	0.915	0.915	0.88
80	0.904	0.912	0.919	0.900	0.900	0.898	0.88

TABLE II. Power and Feedback History in Khalil-Yarlagadda LMFBR LOF Calculations, Homogeneous Core

			Reactivity Ramp Rates, $/sec.														
			Sodium Voiding			Fuel Motion					Axial Fuel Expansion			Doppler			
Time, Sec.	Power	Net Reactivity $	Higher Power Channels	Lower Power Channels	Total	Higher Power Channels	Lower Power Channels	Total	Clad Motion	Total of Sodium, Fuel, and Clad	Higher Power Channels	Lower Power Channels	Total	Higher Power Channels	Lower Power Channels	Total	Total of Axial Expansion and Doppler	Net
10.2700	1.1	0.077																
10.4406	3.2	0.692	4		4					4								
10.571	12	0.879	5		5					5	-1	-1	-2			-2	-4	1
10.6725	37	0.933	5	4	9					9	-2	-2	-4			-4	-8	1
10.6899	55	0.957	9	4	13					13	-2	-5	-7			-5	-12	1
10.6995	222	1.012	16	10	28	13		13		41		-10	-10	-6	-6	-12	-21	20
10.7011	405	1.034	16	21	37	19	3	22		59		-15	-15	-15	-15	-30	-45	14
10.7031	1134	1.046	16	29	95	31	13	44		89		-18	-18	-29	-35	-64	-72	17
10.7039	1585	1.035	13	46	59	44	44	88		147		-27	-27	-71	-2	-143	-170	-23
10.7042	1900	1.077	14	182	196	53	88	141		337		-15	-15	-109	-73	-182	-197	140
10.7048	2896	1.033			67	77	116	193		260		-16	-16	-176	-143	-319	-335	-75
10.7050	3001	0.998			60	80	15	95		145		-12	-12	-164	-154	-318	-330	-185
10.7056	2099	0.921			77	107	20	127	2	206				-175	-157	-332	-332	-126
10.7072	715	0.935			88	104	-63	38	12	138				-63	-68	-131	-131	7
10.7101	27	0.497			118	-211	-176	-387	101	-168						49	49	-119

TABLE III. Feedback History in Khalil and Yarlagadda LMFBR LOF Calculations, Quasi-Homogeneous Core (R6)

Time, Sec.	Power	Net Reactivity $	Reactivity Ramp Rates, $/sec.														
			Sodium Voiding			Fuel Motion				Total of Sodium, Fuel, and Clad	Axial Fuel Expansion			Doppler			Total of Axial Expansion and Doppler	Net
			SPA Channels	LPA Channels	Total	SPA Channels	LPA Channels	Total	Clad Motion		SPA Channels	LPA Channels	Total	SPA Channels	LPA Channels	Total		
10.1800	1.06	0.0918																
10.2700	1.30	0.2646	2							2								2
10.3700	1.84	0.4708	2							2								2
10.5900	3.1	0.6346	2							2								2
10.9500	5.8	0.7083	2							2	-1		-1			-1	-2	0
11.2342	61	0.9590	1	2	3					3						-1	-1	2
11.2420	148	0.9952	2	8	10	7		7	2	19	-3	-2	-5	-3	-6	-9	-14	5
11.2439	186	1.0001	2	11	13	14		14	2	29	-4	-4	-8	-7	-10	-17	-25	4
11.2461	280	1.0115	1	11	12	19		19	2	33	-6	-5	-11	-6	-12	-18	-29	4
11.2480	436	1.0203	2	11	13	28		28	1	42	-7	-8	-15	-4	-17	-21	-36	6
11.2489	537	1.0169	1	11	12	31		31	1	44	-11	-9	-20	-5	-21	-26	-46	-2
11.2502	679	1.0071	2	14	16	29		29	3	48	-8	-11	-19	-11	-23	-34	-53	-5
11.2525	767	0.9953	1	16	17	25		25	6	48	-1	-7	-8	-21	-26	-47	-55	-7
11.2536	788	0.9968	1	19	20	25	3	26	10	58				-26	-26	-52	-52	6
11.2548	895	1.0095	1	16	19	18	13	31	12	62				-28	-22	-50	-50	12
11.2559	984	0.9923	0	17	17	6	15	21	15	53				-40	-32	-72	-72	-19
11.2563	971	0.9822	2	18	20	-32	21	-11	21	30				-10	-27	-37	-37	-7
11.2573	676	0.9042	-8	30	22	-79	19	-60	24	-14				-28	-38	-66	-66	-80
11.2588	100	0.6821	-2	21	24	-240	47	-193	38	-145				-5	-18	-23	-23	-168

TABLE IV. Power and Reactivity History in Khalil-Yarlagadda LMFBR LOF Calculations, Heterogeneous Case

Time, Sec.	Power	Net Reactivity $	Reactivity Ramp Rates, $/sec.											
			Sodium Voiding	Fuel Motion	Clad Motion	Total of Sodium, Fuel and Clad	Axial Fuel Expansion			Doppler			Total of Axial Fuel Exp. and Doppler	Net
							Driver Channels	Inner Blanket Channels	Total	Driver Channels	Inner Blanket Channels	Total		
10.9600	1.02	0.1145												
11.3299	2.5	0.6106												
11.9565	4.6	0.6815												
12.1722	11.6	0.8223												
12.1972	22.6	0.9036	1		5	6	-1		-1			-2	-3	3
12.2112	33	0.9266	1		7	8	-3	1	-2			-3	-5	3
12.2304	54	0.9514	1		7	8	-3		-3			-1	-4	4
12.2561	57	0.9565	-1	4	2	5	-2	1	-1			-4	-5	0
12.2614	107	0.9823	0	13	0	13	-2	1	-1	-4	-4	-8	-9	4
12.2629	147	1.0081	6	20	0	26	-3	2	-1	-2	-7	-9	-10	16
12.2644	249	1.0201	6	29	-7	28	-4	3	-1	-10	-9	-19	-20	8
12.2656	405	1.0403	3	40	-8	35	-7	6	-1	-3	-15	-18	-19	16
12.2667	661	1.0431	2	51	-4	49	-11	10	-1	-19	-26	-45	-46	3
12.2682	1116	1.0249	1	67	-2	66	-13	15	2	-39	-41	-80	-78	-12
12.2707	1748	1.0096	2	100	-2	104	-3	24	21	-73	-59	-132	-111	-7
12.2727	1757	0.9541	2	63	12	77		21	21	-73	-48	-121	-100	-23
12.2744	19	0.1575	1	-454	79	-374		7	7	-13	-17	-30	-23	-397

TABLE V. Reactivity Components at Peak Net Reactivity in Khalil and Yarlagadda LMFBR LOF Calculations

Time	Net	Reactivity Components, $											
		Sodium Voiding			Fuel Motion			Clad Motion	Axial Fuel Expansion				Doppler
		Higher Power (or SP) Assemblies	Lower Power (or LP) Assemblies	Total	Higher Power Channels	Lower Power Channels	Total		Higher Power Channels	Lower Power Channels	Inner Blanket	Total	
						Homogeneous Case							
Total Core Worth		3.072	2.566	5.638									
10.7042	1.077	2.865	0.600	3.465	0.189	0.092	0.281	0.0	-0.746	-0.403	--	-1.1492	-1.521
						Quasi-Homogeneous (R6A) Case							
Total Core Worth		7.941	1.618	4.559									
11.2479	1.022	1.556	1.086	2.642	0.178	0.0	0.175	0.037	-0.628	-0.180	--	-0.808	-1.024
						Heterogeneous Case							
Total Core Worth		2.132	-0.104	2.998									
12.2667	1.045	2.158	-0.049	2.192	0.362	0.0	0.362	0.514	-0.730	-0.196	0.148	-0.778	-1.246

Distribution for NUREG/CR-4240 Vol. I (ANL-85-23 Vol. I)

Internal:

C. E. Till
R. A. Scharping
R. J. Armani
R. Avery
T. H. Bauer
I. Bornstein/
A. B. Klickman
C. E. Dickerman
F. E. Dunn
R. A. Valentin/L. Baker
S. H. Fistedis
P. L. Garner
E. Gelbard
H. H. Hummel (6)
Kalimullah
J. M. Kramer
L. G. LeSage
D. J. Malloy
A. P. Olson
P. Pizzica
F. G. Prohammer
D. Rose/A. J. Goldman/
J. F. Marchaterre
R. Sevy
J. J. Sienicki
B. J. Toppel
J. B. van Erp
D. Weber
H. M. Domanus
V. L. Shah
B. C-J. Chen
R. W. Lyczkowski
W. T. Sha
S. G. Carpenter
H. F. McFarlane
D. H. Shaftman
A. Travelli
ANL Contract File
ANL Patent Dept.
ANL Libraries (2)
TIS Files (3)

External:

USNRC, Washington, for distribution per R7 (250)
DOE-TIC, Oak Ridge (2)
Manager, Chicago Operations Office, DOE
B. D. Shipp, DOE-CH
Applied Physics Division Review Committee:
J. F. Jackson, Los Alamos National Lab., P. O. Box 1663, Los Alamos, N. M. 87545
W. E. Kastenberg, U. California, Los Angeles, Calif. 90024
N. J. McCormick, U. Washington, Seattle, Wash. 98195
D. A. Meneley, U. New Brunswick, Fredericton, N. B., Canada
J. E. Meyer, Massachusetts Inst. Technology, Cambridge, Mass. 02139
A. E. Wilson, Idaho State U., Pocatello, Id. 83209
E. L. Zebroski, Electric Power Research Inst., P. O. Box 10412, Palo Alto, Calif. 94303
Components Technology Division Review Committee:
P. Alexander, Flopetrol Johnston Schlumberger, P. O. Box 36369, Houston, Tex. 77236
D. J. Anthony, General Electric Co., 175 Curtner Ave., San Jose, Calif. 95125
A. A. Bishop, U. Pittsburgh, Pittsburgh, Pa. 15261
B. A. Boley, Northwestern U., Evanston, Ill. 60201
F. W. Buckman, Delian Corp., Monroeville, Pa. 15146
R. Cohen, Purdue U., West Lafayette, Ind. 47907
J. Weisman, U. Cincinnati, Cincinnati, O. 45221
C. Erdman, Texas A&M U., College Station, Tex. 77843
R. Lancet, Rockwell International Corp., P. O. 309, Canoga Park, Calif. 91304
K. O. Ott, Purdue U., West Lafayette, Ind. 47907

NRC FORM 335 (2-84) NRCM 1102 3201, 3202

U.S. NUCLEAR REGULATORY COMMISSION

BIBLIOGRAPHIC DATA SHEET

SEE INSTRUCTIONS ON THE REVERSE

1. REPORT NUMBER (Assigned by TIDC, add Vol. No., if any)

ANL-85-23 Vol. I
NUREG/CR-4240 Vol. I

2. TITLE AND SUBTITLE

Physics of Reactor Safety Quarterly Report
January-March 1985

3. LEAVE BLANK

4. DATE REPORT COMPLETED

MONTH: May — YEAR: 1985

5. AUTHOR(S)

Applied Physics Division
Components Technology Division

6. DATE REPORT ISSUED

MONTH: June — YEAR: 1985

7. PERFORMING ORGANIZATION NAME AND MAILING ADDRESS (Include Zip Code)

Argonne National Laboratory
9700 S. Cass Avenue
Argonne, IL 60439

8. PROJECT/TASK/WORK UNIT NUMBER

9. FIN OR GRANT NUMBER

A2015
A2045

10. SPONSORING ORGANIZATION NAME AND MAILING ADDRESS (Include Zip Code)

Division of Reactor Safety Research
Office of Nuclear Regulatory Research
U.S. Nuclear Regulatory Commission
Washington, D.C. 20555

11a. TYPE OF REPORT

Quarterly

b. PERIOD COVERED (Inclusive dates)

January-March 1985

12. SUPPLEMENTARY NOTES

13. ABSTRACT (200 words or less)

This quarterly progress report summarizes work done during the months of January-March 1985 in Argonne National Laboratory's Applied Physics and Components Technology Divisions for the Division of Reactor Safety Research in the U.S. Nuclear Regulatory Commission. The work in the Applied Physics Division includes reports on reactor safety modeling and assessment by members of the Reactor Safety Appraisals Section. Work on reactor core thermal-hydraulics is performed at ANL's Components Technology Division, emphasizing 3-dimensional code development for LMFBR accidents under natural convection conditions. An executive summary is provided including a statement of the findings and recommendations of the report.

14. DOCUMENT ANALYSIS - a. KEYWORDS/DESCRIPTORS

LMFBR Safety
Core Disruptive Accident Analysis
CRBR Licensing
Reactor Core Thermal Hydraulics
Natural Convection Core Cooling

b. IDENTIFIERS/OPEN-ENDED TERMS

15. AVAILABILITY STATEMENT

unlimited

16. SECURITY CLASSIFICATION (This page)

unclassified

(This report)

unclassified

17. NUMBER OF PAGES

26

18. PRICE